JOURNAL OF MATERIALS SCIENCE 23 (1988) 2485–2494

Grain boundary precipitation in Magnox AL80

Y. P. LIN*
H. H. Wills Physics Laboratory, University of Bristol, Tyndall Avenue, Bristol BS8 1TL, UK
G. C. SMITH
Department of Materials Science and Metallurgy, University of Cambridge, Pembroke Street, Cambridge CB2 3QZ, UK

Grain boundary precipitates in Magnox AL80 (Mg–0.8% Al) formed after certain heat treatments have been identified as magnesium hydride, MgH_2. The solvus temperature for the precipitates was found to be in the range of 300 to 350° C. Ageing at 250° C resulted in overall precipitate growth accompanied by the formation of some grain boundary cavities. Cavities were also formed when hydride precipitates were reheated to higher temperatures. The solvus temperature and the behaviour of the precipitates during ageing at 250° C and subsequent heating to higher temperatures are discussed in terms of the magnesium–hydrogen system.

1. Introduction

Magnox AL80, a magnesium-based alloy containing nominally 0.80 wt % Al and 50 p.p.m. by weight of beryllium, is used as the fuel-element cladding material in gas–graphite nuclear reactors. The material is essentially single-phase, although observations of second-phase particles have been previously reported [1–3]. Harris [4] showed that nucleation of grain boundary cavities at second-phase particles ranging from 20 to 200 nm was possible under certain service conditions. In Magnox grain interiors, Lisowyj [3] observed five species of particles of sizes less than 35 nm, namely Mg_2Si, MgO, $FeBe_5$, $MnAlBe_4$ and $MgBe_{13}$. Of more interest to the elevated-temperature mechanical properties are the much larger, micrometer-sized intergranular precipitates which have been observed in some batches of Magnox AL80 after specific heat treatments [2, 3]. It was thought that these might also be $MgBe_{13}$ [3] but subsequent observation by Slack, quoted by Ross [5], of similar grain boundary precipitates in pure magnesium and beryllium-free Magnox AL80 led to the suggestion that the precipitates were magnesium hydride. This was largely confirmed as a result of hydrogen detection by a laser-induced mass analysis (LIMA) investigation although a positive identification of the precipitates was not achieved [5]. In the present work, various aspects of the grain boundary precipitation phenomenon in Magnox AL80 have been investigated and also further evidence obtained about the nature of the precipitates.

2. Materials and experimental details

Three batches of Magnox AL80, supplied as either 31.8 mm (1.25 in.) or 28.6 mm (1.125 in.) rods, were used. The chemical analyses of these casts are given in Table I.

Following heat treatments in air, samples for metallographic examination were sectioned and mounted in cold-setting plastic resin and ground on progressively finer grades of silicon carbide paper. Final polishing was performed using Brasso metal polish on a rotating pad of Selvyt napped cloth. A solution of 10% nitric acid in methanol was normally used to reveal the grain structure.

Impact fracture surfaces of notched round specimens were produced using a Hounsfield impact testing machine. Fracture surfaces were examined in an ISI 100A scanning electron microscope (SEM) equipped with a Link System 840 energy dispersive spectroscopy (EDS) attachment.

A two-stage replication technique was used to extract grain boundary precipitates from impact fracture surfaces. Thick cellulose acetate strip was softened with acetone and pressed on to the fracture surface. When dry, the replica was peeled off and carbon evaporated on to it. The relevant portion of the replica was then cut off and the backing cellulose acetate replica dissolved away in acetone. The carbon replica could then be scooped on to a copper grid and examined either in a Jeol EM200 or a Philips EM400 transmission electron microscope (TEM). The latter was also equipped with EDS facilities.

3. Results and discussion

3.1. Formation of grain boundary precipitates

The precipitates were observed most readily after a furnace-cool to room temperature (RT) from a solution treatment temperature of 580° C, when large isolated particles were formed (Fig. 1). Usually, not more than two or three precipitates would be present on any one boundary, and some boundaries did not have any; a variation which was probably a result of the variation in misorientation across the grain boundaries. Stringers of smaller precipitates outlining some boundaries, as in Fig. 2, were observed after a water-quench from 580° C followed by ageing at 250° C. Such precipitation behaviour would be consistent with a precipitation system where the solute solubility decreases with decreasing temperature. To

* *Present address*: Department of Materials Science and Engineering, McMaster University, Hamilton L8S 4LT, Canada.

0022–2461/88 $03.00 + .12

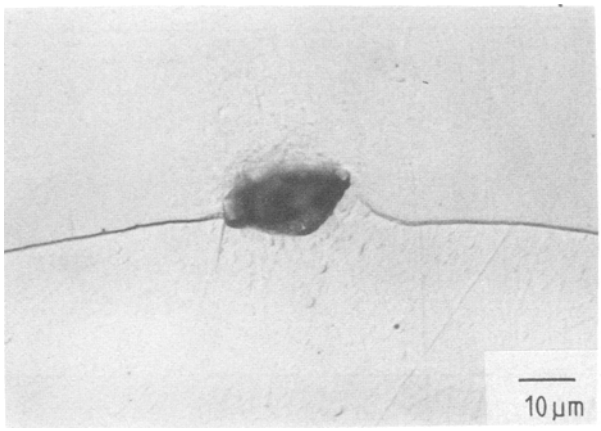

Figure 1 Typical grain boundary precipitate formed after a furnace-cool from 580° C to RT.

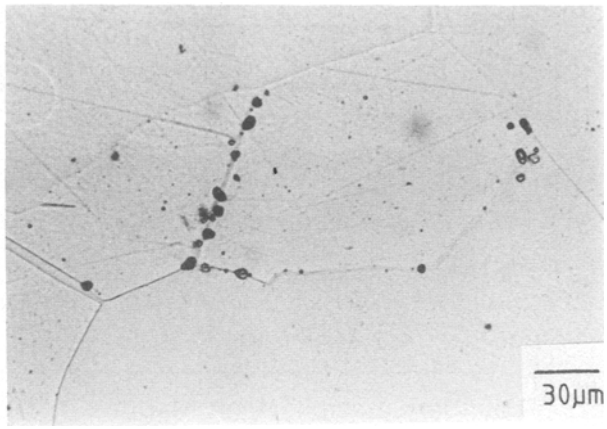

Figure 2 Grain boundary precipitate formed after ageing at 250° C for 20 h.

estimate the solvus temperature, specimens were examined metallographically after three different heat treatments:

(i) Holding treatments in which samples were furnace-cooled from the solution treatment temperature of 580° C to various intermediate temperatures, held for 20 h and quenched to RT.

(ii) Ageing treatments in which samples were water-quenched from 580° C to RT and then aged at various temperatures for 20 h and, finally, water-quenched to RT.

(iii) Reheating treatments in which samples previously furnace-cooled from 580° C to RT were reheated to various temperatures for 20 h and, finally, water-quenched to RT.

Specimens from casts A, B and C were used and the solvus temperatures deduced from the different heat treatments were all in the range 300 to 350° C.

To estimate the precipitate volume fraction, polished and etched sections were examined using a Cambridge Instrument Quantimet image analyser. The image editor was employed to ensure that only grain boundary precipitates were analysed. The specimens were previously furnace-cooled from 580° C to RT so that isolated large grain-boundary precipitates were present. For each sample, a total area of about 40 mm^2 was examined and typically about 300 precipitates were counted. An average area fraction of about 0.02% was found and taken as an approximate value of the volume percentage of the precipitates present.

3.2. Ageing behaviour

The development of the grain boundary precipitates during ageing at 250° C was monitored by the examination of impact fracture surfaces. Specimens were water-quenched from 580° C to RT, aged at 250° C for various lengths of time and then water-quenched again to RT. With no ageing at 250° C, i.e. as-quenched, although precipitates could not be resolved on the intergranular facets, shallow dimples (Fig. 3) typical of fracture by micro-void coalescence were nevertheless present. This suggested that fine-grain boundary precipitates may already have formed during the water-quench from 580° C and holding at RT.

The precipitates developed rapidly during ageing and were easily observed after a 1 min ageing treatment. Figs 4a, b, c and d show typical micrographs of samples aged at 250° C for 1 min, 5 h, 24 h and 16 days, respectively. For the longer times, agglomeration of smaller precipitates was often found as in Fig. 4d, which also shows the shallow dimples typical of as-quenched samples in regions between the precipitates. Fig. 5 is a plot as a function of time of the largest observed precipitate in each sample, after examination of several boundary facets in the SEM, and demonstrates the coarsening which occurred during ageing.

Further examination of the fracture surfaces of samples subjected to prolonged ageing, particularly with ageing times greater than 24 h, showed that while some boundaries showed the presence of large precipitates (e.g. Figs 4c and d), there were also some boundaries which showed large dimples or voids (5 μm or more in size) which contained precipitates which were much smaller than the voids. These small precipitates were usually equiaxed and often faceted. Examples are shown in Figs 6a and b. Such a configuration of precipitates in dimples was unlike than seen on the fracture surfaces shown in Figs 4a to d, where the dimple size was of the order of the precipitate size. The rounded appearance and the rounded

TABLE I Chemical analyses of Magnox AL80 casts

Cast	Content (wt %)								
	Al	Si	Mn	Fe	Ca	Zn	Be	H (p.p.m.)	Mg
A	0.83	0.008	0.006	0.003	< 0.005	0.006	0.005	11	Bal.
B	0.82	0.005	0.006	0.005	< 0.005	0.007	0.005	11	Bal.
C	0.84	0.005	0.007	0.005	< 0.005	0.002	0.004	9	Bal.

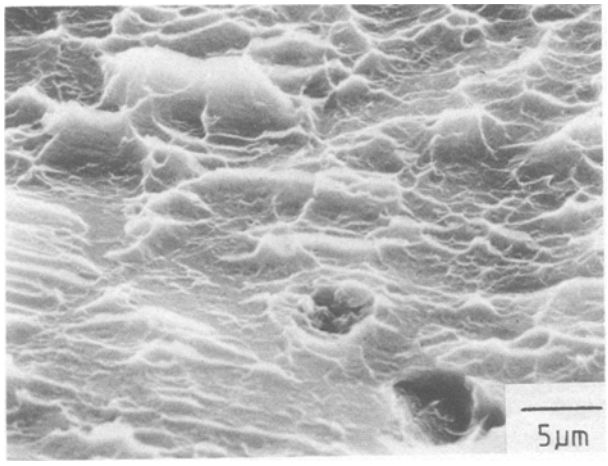

Figure 3 Grain boundary facet in a sample quenched to RT from 580° C.

corners between facets of the small precipitates ruled out the possibility that they were fragments of fractured large precipitates, e.g. Fig. 4d shows a cracked particle. Also, the walls of the large dimples or voids often exhibited facets (Figs 6a and b), an effect which was unlikely to have been produced by the impact fracture.

Examination of polished but unetched sections in the SEM revealed the presence of cavities as well as precipitates on some grain boundaries (Fig. 7). However, this could not be taken as conclusive evidence for the existence of voids prior to impact fracture, since some of the cavities might have been due to precipitates falling out during surface preparation.

3.3. Anomalies during post-ageing treatments

Grain boundary cavities were also observed in quenched-and-aged (24 h at 250° C) samples after they had been reheated to 350 or 450° C for between 0.5 and 2 h and finally water-quenched to RT. Examples of such cavities are shown in Fig. 8. The cavities were smooth and rounded (Fig. 8b) or faceted (Fig. 8c). Both types were usually present in the same sample, although the faceted type appeared to be more abundant in samples subjected to longer reheating times. The correspondence of void sites with prior grain boundary precipitates was demonstrated by a short reheating of 10 min at 350° C of samples previously aged at 250° C. After such a treatment, residual small precipitates were observed situated inside relatively large dimples (Fig. 9).

On polished but unetched sectioned surfaces of samples given longer reheating times, cavities were visible which appeared to outline boundary traces (Fig. 10). However, the number of such boundary traces per unit area was much lower than that of boundary traces decorated by precipitates in the original quenched-and-aged (at 250° C) samples, (Fig. 2). This suggested that not all precipitates gave rise to cavities when they were reheated to higher temperatures. Since no precipitates would be expected

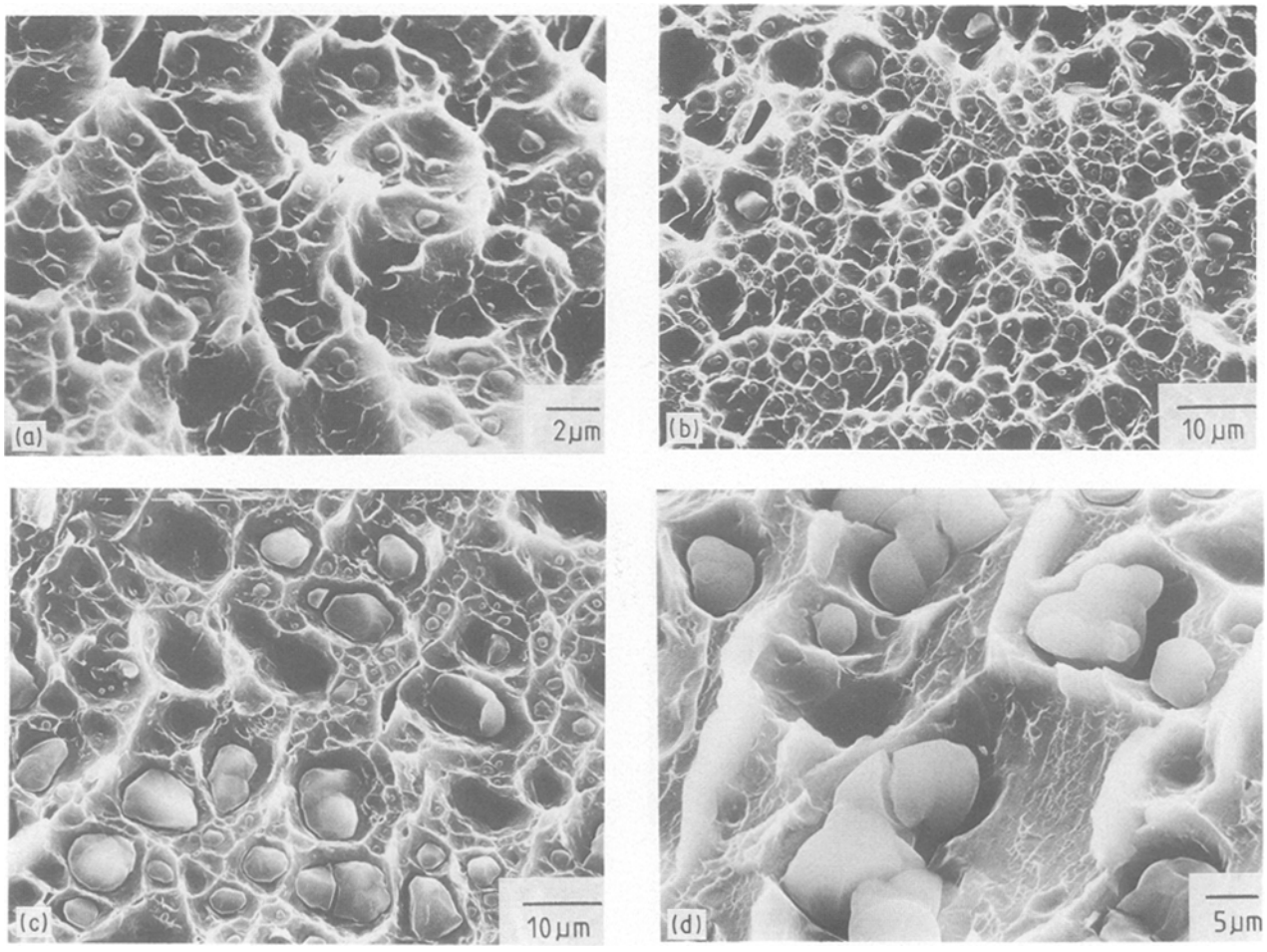

Figure 4 (a) Grain boundary precipitates in a sample aged at 250° C for 1 min. (b) As (a) but after 5 h at 250° C. (c) As (a) but after 24 h at 250° C. (d) As (a) but after 16 days at 250° C.

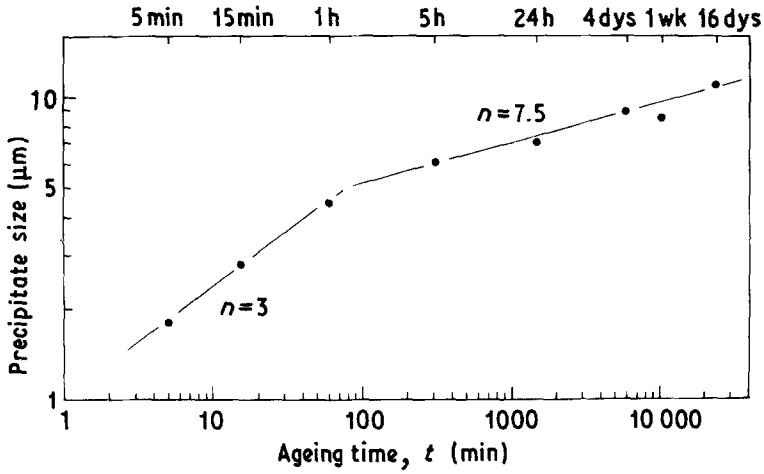

Figure 5 Variation of observed maximum precipitate size with ageing time at 250° C.

at the reheating temperatures of 350 or 450° C, which are above the solvus, the possibility of precipitates falling out during surface preparation did not arise. These observations thus indicated that precipitates formed during ageing at 250° C could be removed as would be expected by reheating to higher temperatures, but that this resulted initially in cavities left behind on some boundaries. Cavities were also observed, although only rarely, on grain boundary facets produced by the impact fracture of furnace-cooled samples which had been reheated at 450° C for 2 h prior to fracture at room temperature.

Fig. 11a and b show features on the impact fracture surface of a sample which, after a reheating treatment at 450° C for 2 h, had been re-aged at 250° C. The precipitates have a somewhat different morphology, with the appearance of hollow capsules (Fig. 11a). Such a morphology would be consistent with nucleation at the cavity walls to produce a shell of precipitate. Fig. 11b shows a region of extensive linkage of cavities so that only a very limited contact area existed between the two component grains prior to impact fracture. Such extensive boundary cavitation clearly would have a pronounced detrimental effect on the strength of the boundary.

3.4. Silicon-rich particles

In addition to the large particles discussed so far, others, typically a few hundred nanometres in size, were also observed on dimple walls, e.g. Figs 6a, 6b, 8b, 8c, 11a and 11b. EDS examination showed the particles to be rich in silicon, although occasional ones were found to be rich in manganese. However, since Mg_2Si has been identified as a precipitate species in Magnox AL80 [3], it is considered that the majority of these small particles were Mg_2Si. The size difference between such particles and the dimples, and the frequent presence of more than one particle per dimple, suggested that they did not play an active role in the impact fracture process.

3.5. Identification of the grain boundary precipitates

Carbon replicas containing the main grain boundary precipitates extracted from impact fracture surfaces were examined in TEM (Fig. 12). When analysed using EDS, the spectrum (Fig. 13), which would not include any complication from the mainly magnesium matrix, showed only the magnesium $K\alpha$ peak apart from the copper and platinum peaks which were due to the specimen holder and supporting grid. The analysis thus suggested that the precipitates were a compound of magnesium with light element(s) which could not be detected using EDS, i.e. elements with atomic numbers less than 11. A likely possibility was hydrogen, in view of the earlier work mentioned in the introduction [5].

Selected-area electron diffraction (SAED) patterns

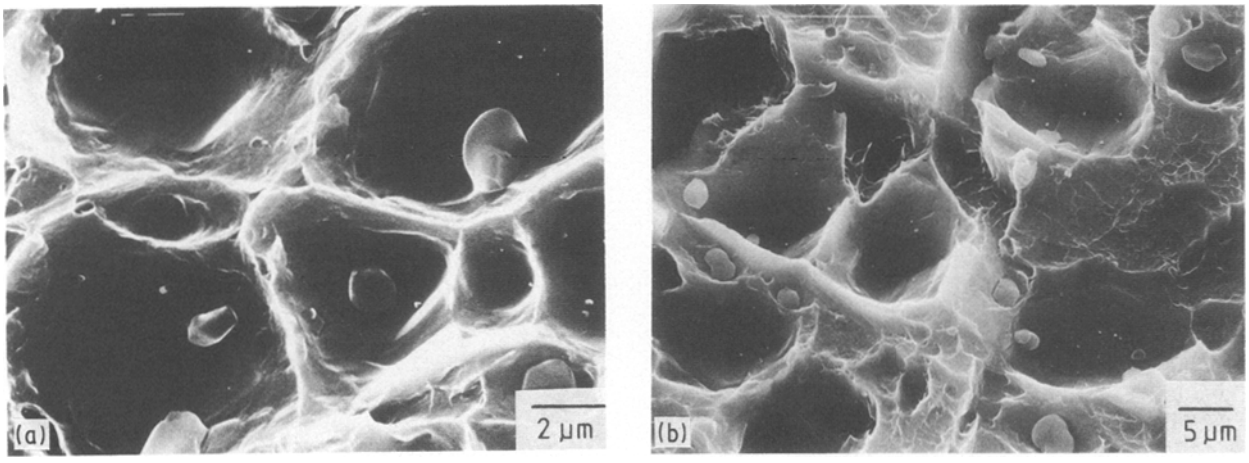

Figure 6 (a) Impact fracture surface of a sample after 7 days at 250° C, showing small precipitates inside large cavities. (b) As (a) but from sample aged at 250° C for 16 days.

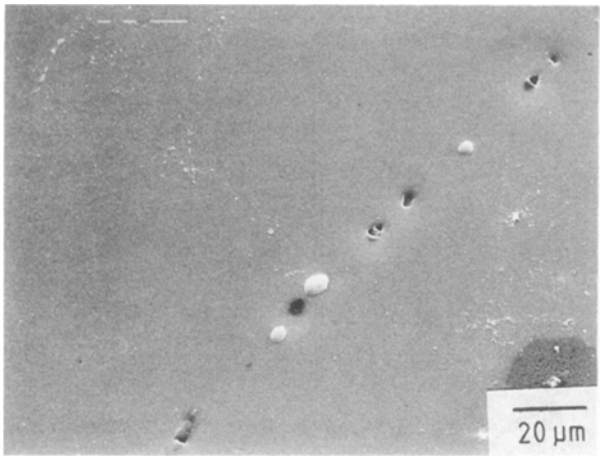

Figure 7 Polished but unetched section of a sample aged at 250° C for 16 days.

were therefore obtained from the extracted precipitates. The operating voltage of the microscope was reduced to 80 kV, so that serious beam damage effects were avoided for a sufficiently long period of time to allow diffraction patterns to be recorded. Also, as each precipitate often consisted of more than one grain, it was necessary to use a small selected-area aperture (5 μm) to ensure that only one grain gave rise to the observed diffraction pattern. However, the majority of the particles were opaque to the electrons, so that diffraction patterns could be obtained only from thin particles or edges of relatively thin particles.

The SAED patterns obtained could be indexed in terms of the tetragonal structure of MgH_2 which belongs to the space group $P4_2/mnm$ with $a = 0.45025$ nm and $c = 0.30123$ nm and with two magnesium atoms at (0, 0, 0) and $(\frac{1}{2}, \frac{1}{2}, \frac{1}{2})$ and four hydrogen atoms at $(x, x, 0)$, $(\bar{x}, \bar{x}, 0)$, $(\frac{1}{2} + x, \frac{1}{2} - x, \frac{1}{2})$ and $(\frac{1}{2} - x, \frac{1}{2} + x, \frac{1}{2})$ with $x = 0.306$ [6, 7]. In all, two patterns of the [1 0 0] zone, two of [1 1 0], nine of [1 1 1], six of [1 0 1] and three of [0 0 1] were obtained and Figs 14a–e show patterns corresponding respectively to these zones of MgH_2. From the [1 0 0] and [1 1 0] patterns (Figs 14a and b, respectively) the c/a ratio for the grain boundary precipitates is deduced to be 0.667 ± 0.005, which is in close agreement with the value of 0.669 for MgH_2 and MgD_2 obtained using X-ray and neutron diffraction methods [6, 7]. Although magnesium forms several compounds with other elements with atomic numbers less than 11, none of these compounds have tetragonal structures near to an axial ratio of 0.667.

There is, however, one point worthy of note. Reflections due to the hydrogen superstructure are expected to be weak in comparison with the magnesium reflections, and for the [1 1 0] and [1 0 1] zones, alternating strong/weak/strong rows of reflections are expected, as has been observed previously [8]. Such a variation in intensity between rows of reflections was observed for the [1 0 1] patterns [Fig. 14d). It was also found for one [1 1 0] pattern, but another [1 1 0] pattern showed some reflections with surprisingly strong intensities (Fig. 14b). At present there is no explanation for this difference in behaviour.

Previous TEM examination of magnesium foils containing MgH_2 had shown that decomposition of MgH_2 due to electron beam irradiation resulted in the formation of small hydrogen gas bubbles [8, 9]. However, in the present work, although beam damage was evident in the diffraction patterns after intense beam irradiation, no gas bubbles would be expected from particles contained on a replica.

The present electron diffraction evidence is in agreement with the earlier identification of the precipitates as magnesium hydride, from the results of a LIMA investigation of Magnox micro-specimens and frac-

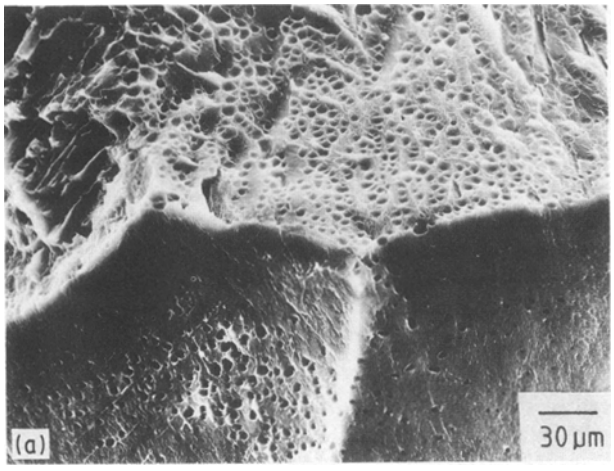

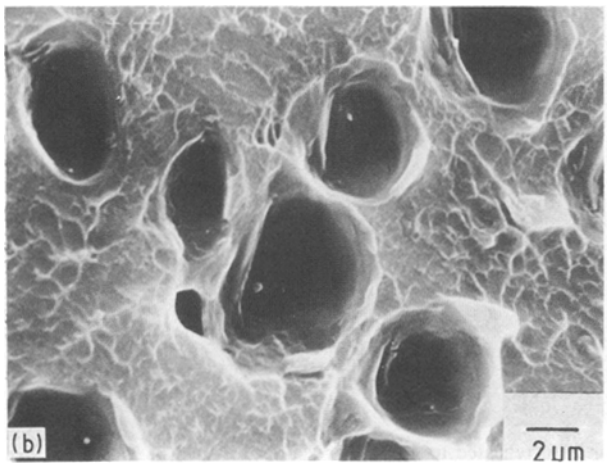

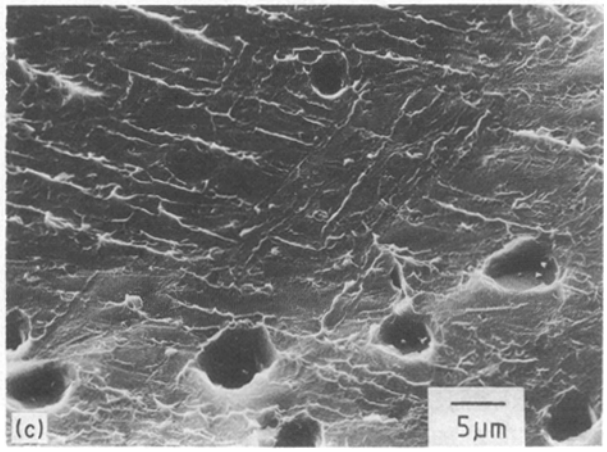

Figure 8 (a, b) Impact fracture surface of sample reheated to 450° C for 2 h after ageing at 250°C for 24 h, showing cavities on grain boundary facets. (c) As (a) but from sample reheated for 8 h at 450° C.

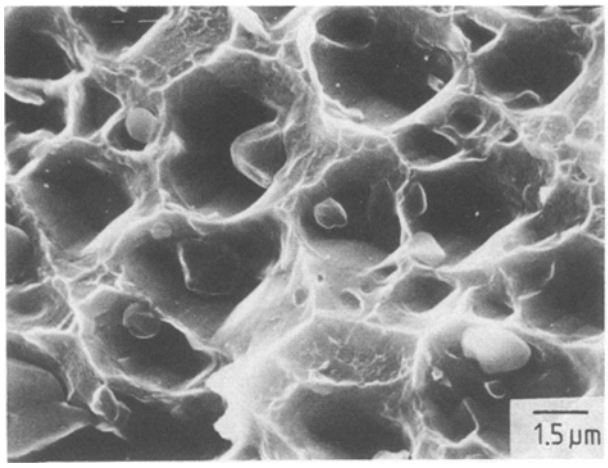

Figure 9 Impact fracture surface of a sample reheated to 350° C for 10 min following ageing at 250° C.

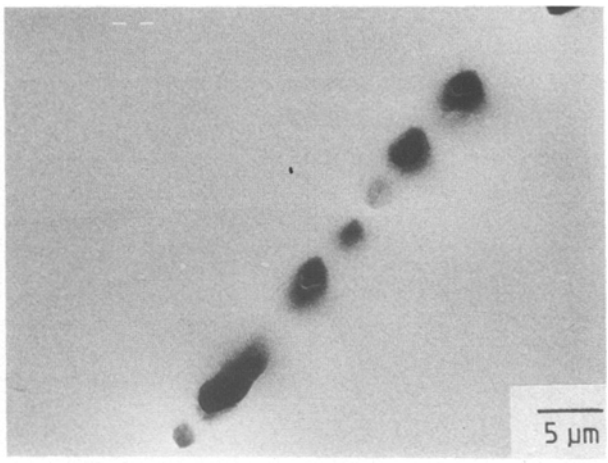

Figure 10 Polished but unetched section of a sample reheated to 350° C for 2 h following ageing at 250° C, showing presence of cavities.

ture surfaces [5]. The LIMA instrument operates by firing a laser pulse on to the sample and analysing the evaporated atoms, and is capable of detecting hydrogen and other light elements which are not easily detected by other analytical instruments. The results showed the presence of hydrogen in the precipitates on grain boundaries, but not elsewhere on the boundaries or within the grains.

3.6. The magnesium–hydrogen system

With the grain boundary precipitates identified as MgH_2 and since 0.8 wt % Al is the only major alloying addition in Magnox Al80 (see Table I), some aspects of the precipitation phenomena described earlier can be considered in terms of the magnesium–hydrogen system. Magnesium is an endothermic occluder of hydrogen in dilute concentrations [10, 11] but forms the hydride, MgH_2, exothermically [12]. Fig. 15 shows schematically the pressure–composition isotherms expected for such a metal–hydrogen system. Starting from the origin and up to the limiting solubility at A, the hydrogen is in solid solution in magnesium, while the hydride phase is formed in the plateau region AB. The plateau pressure is also the hydride dissociation pressure for the temperature considered.

For hydrogen entering magnesium to form a solid solution according to the reversible reaction

$$Mg + \frac{x}{2} H_2 \rightleftharpoons Mg_{(xH)}$$

the solubility against pressure isotherms can be written as

$$\ln x = \tfrac{1}{2} \ln P - \frac{\Delta H_1}{RT} + \frac{\Delta S_1}{R} + \ln Z \quad (1)$$

where x is the hydrogen-to-metal atom ratio, P the hydrogen pressure in atmospheres, ΔH_1 the partial molar enthalpy change, ΔS_1 the partial molar entropy change due to non-configurational contributions from magnetic, electronic and vibrational terms, Z the number of available interstitial sites per metal atom, R and T the gas constant and temperature, respectively. The limiting solubility, x_1 is given by

$$\ln x_1 = \frac{\Delta H_2 - \Delta H_1}{RT} - \frac{\Delta S_2 - \Delta S_1}{R} + \ln Z \quad (2)$$

where ΔH_2 and ΔS_2 are respectively the partial molar enthalpy and entropy changes for the reversible hydride forming reaction

$$Mg + \frac{x}{2} H_2 \rightleftharpoons MgH_x$$

Values of ΔH_1, ΔH_2, ΔS_1 and ΔS_2 have been reported [10–16] and are collated in Table II. The values are reasonably consistent except for one rather high value of ΔH_1 [15] which has been suggested to be the difference between the enthalpy of hydriding and

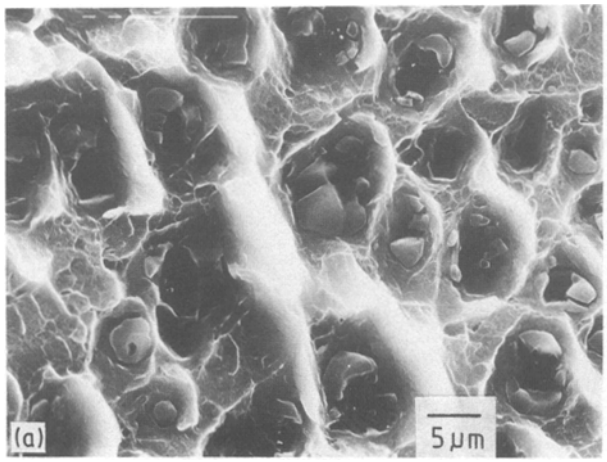

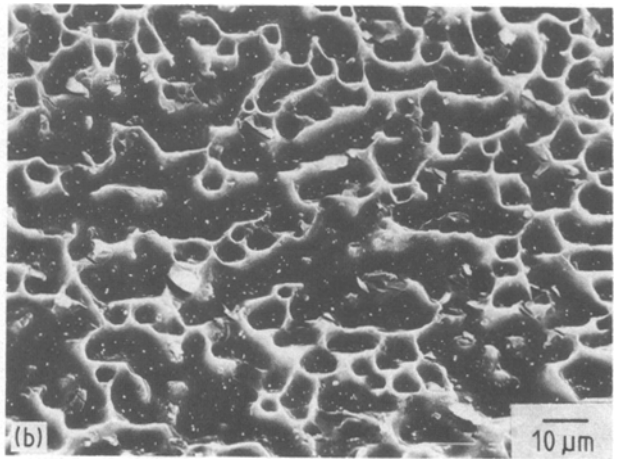

Figure 11 (a, b) Impact fracture surface of a sample aged at 250° C for 24 h, reheated to 450° C for 2 h and re-aged at 250° C for 24 h.

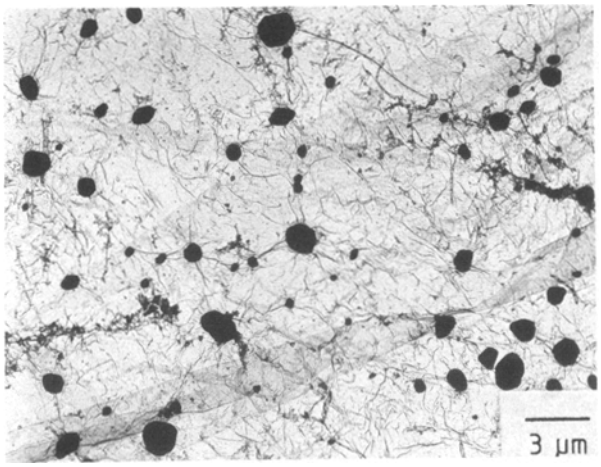

Figure 12 Carbon replica containing grain boundary precipitates extracted from impact fracture surface of a sample aged at 250° C for 24 h.

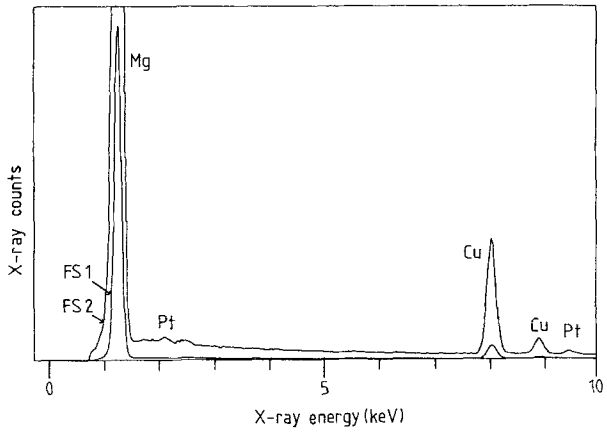

Figure 13 EDS spectrum (with two different vertical scales) obtained from precipitate on carbon replica. Full scales FS1 = 32000, FS2 = 4000.

of solution [17]. For the present purpose, however, this high value of ΔH_1 has not been included for the evaluation of a mean value of ΔH_1. The value of Z depends on the location of hydrogen in magnesium, such that $Z = 1$ for hydrogen at octahedral interstices and $Z = 2$ for tetrahedral interstices. Experimentally, it was found that implanted hydrogen occupied the tetrahedral interstices in magnesium at low temperatures (below 100 K) but left these sites at higher temperatures; while at temperatures above 230 K, no implanted hydrogen could be retained in the bulk [18]. However, theoretical calculations have shown that hydrogens at octahedral and tetrahedral sites have indistinguishable energies and that diffusion of hydrogen from one octahedral site to another is likely to be via a tetrahedral site [19].

By using $Z = 1$ (i.e. assuming that hydrogen occupies the octahedral interstices in magnesium) and mean values of 21.1 and -37.9 kJ $(\frac{1}{2}\,\text{mol}\,H_2)^{-1}$ for H_1 and H_2 respectively, and -35.5 and $-67.3\,\text{kJ}^{-1}$ $(\frac{1}{2}\,\text{mol}\,H_2)^{-1}$ for S_1 and S_2, respectively (see Table II). Equations 1 and 2 become respectively

$$\ln P = 2 \ln x + 8.54 + (5076/T) \quad (3)$$

$$\ln x_1 = 3.825 - (7097/T) \quad (4)$$

Using these equations, the expected pressure–solubility isotherms and the limiting solubilities (line ABCD) at various temperatures are calculated and plotted in Fig. 16. The expected dissociation pressures (corresponding to the limiting solubilities) at various temperatures are in good agreement with, although in all cases slightly lower than, the reported values [16] which are also plotted.

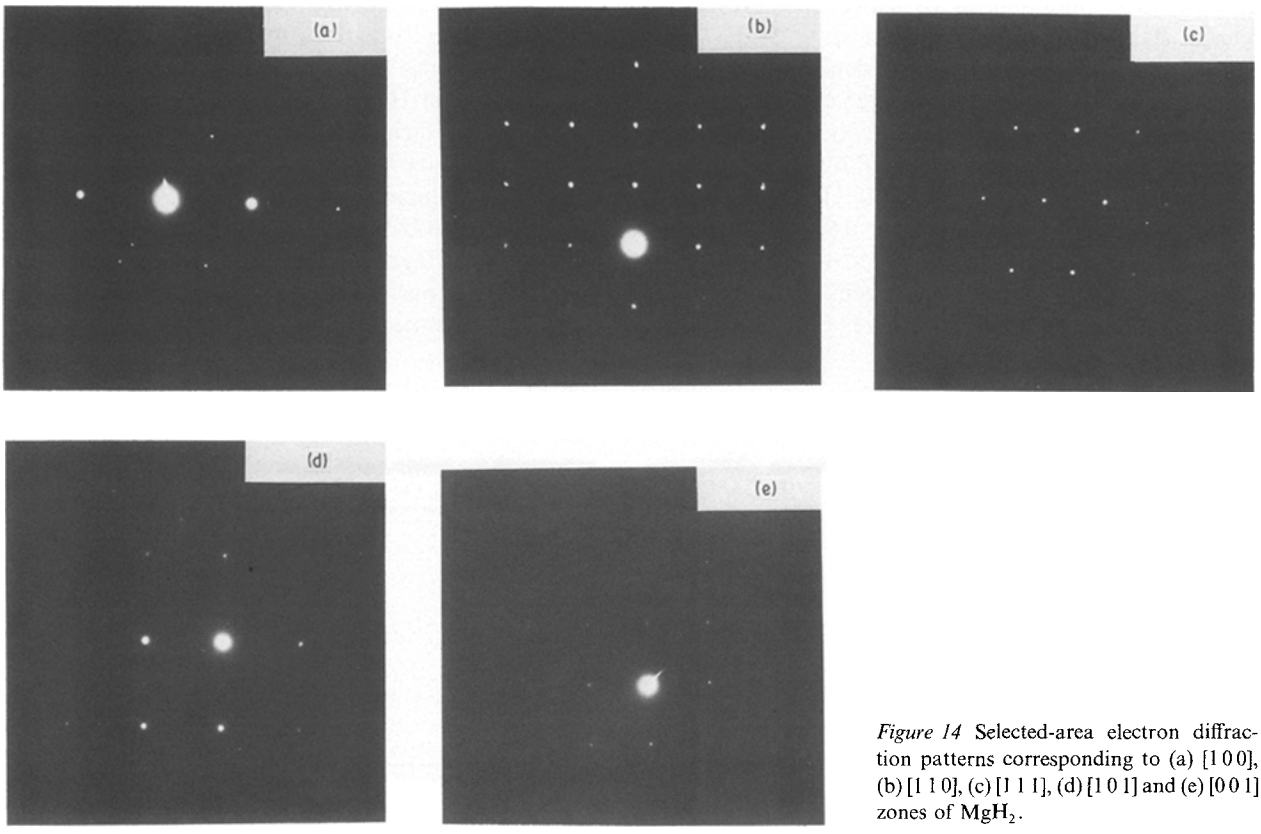

Figure 14 Selected-area electron diffraction patterns corresponding to (a) [1 0 0], (b) [1 1 0], (c) [1 1 1], (d) [1 0 1] and (e) [0 0 1] zones of MgH_2.

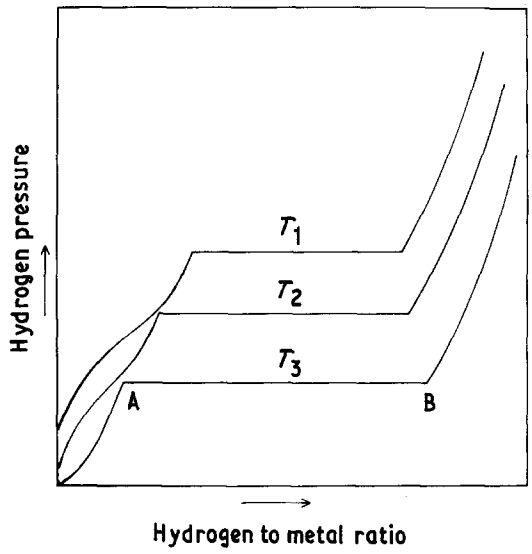

Figure 15 Schematic pressure–solubility isotherms for a metal with which hydrogen forms an endothermic solid solution and an exothermic hydride. $T_1 < T_2 < T_3$.

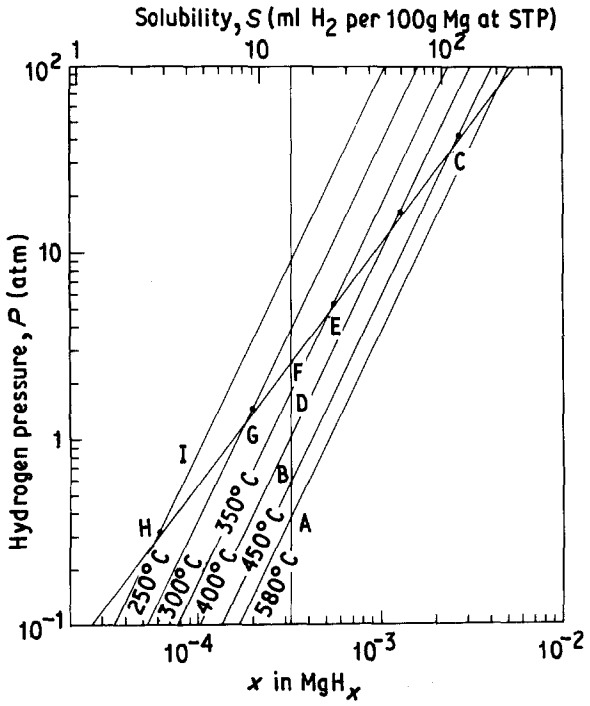

Figure 16 Pressure–solubility isotherms and limiting solubilities predicted using Equations 3 and 4. (●) Dissociation pressure from Huston and Sandrock [16].

From the values of limiting solubilities, the solvus temperature for the hydride precipitation process can be estimated, provided that the hydrogen content of the sample is known. The hydrogen content of the sample in solid solution should be dependent on the external pressure and, since in the present investigation the external hydrogen pressure was always very low, similarly low hydrogen contents in Magnox AL80 would be expected. However, the hydrogen content of Magnox AL80 has been found to be insensitive to the heat treatment environment, and also to remain unchanged during routine heat treatments involving solution treatment and water-quenching [5].

The expected hydrogen content can be estimated from the volume fraction of the grain boundary precipitates, assuming that all the hydrogen is present as MgH_2. By taking the volume fraction to be the same as the area fraction and from the densities [20, 21] of Magnox and MgH_2, respectively 1.75 and 1.45 kg m^{-3}, it can be readily shown that a volume fraction of 0.02% corresponds to about 14 ml hydrogen at STP per 100 g of metal ($x = 3.0 \times 10^{-4}$). This is in the range of typical hydrogen contents of 9 to 17 ml H_2 per 100 g Magnox ($x = 1.95$ to 3.69×10^{-4}) found for Magnox [5]. For a given hydrogen content, which does not change with temperature, the solvus temperature can be estimated as the temperature at which the limiting solubility corresponds to the hydrogen content of the sample, i.e. at lower temperatures hydride will form. Analysis of the present samples (see Table I) showed hydrogen contents of between 9 and 11 ml H_2 per 100 g of Magnox ($x = 1.95$ to 2.38×10^{-4}). Taking a typical value of 12 ml per 100 g and referring to Equation 4 and Fig. 16, it can be seen that a solvus temperature of about 315° C (Point B in Figure 16) would be expected. This is in accord with the present metallographic results showing the solvus temperature to be between 300 and 350° C. Furthermore, from Fig. 16 and Equation 4, this temperature range could arise from hydrogen contents ranging from 9 to 24 ml H_2 per 100 g Magnox ($x = 1.95$ to 5.2×10^{-4}), which covers the range of hydrogen contents for Magnox AL80. This range implies a similar range in the volume fraction of hydride precipitate, so that a batch-to-batch variation in the precipitation behaviour in Magnox AL80 can be explained on the basis of hydrogen-content variations. The above argument assumes that no loss of hydrogen takes

TABLE II Thermodynamic data for the magnesium–hydrogen system*

ΔH_1 (kJ ($\frac{1}{2}$ mol H_2)$^{-1}$)	ΔS_1 (J K^{-1} ($\frac{1}{2}$ mol H_2)$^{-1}$)	ΔH_2 (kJ ($\frac{1}{2}$ mol H_2)$^{-1}$)	ΔS_2 (J K^{-1} ($\frac{1}{2}$ mol H_2)$^{-1}$)	Reference
–	–	−37.2	−67.6	Stampfer *et al.* [12]
24.4†	–	–	–	Popovic and Piercy [10]
21.1	–	–	–	Huang *et al.* [11]
–	–	−38.7	–	Huston and Sandrock [16]
58.0†	–	–	–	Fromageau *et al.* [15]
21.05	−37.7	−37.2	−67.8	Fromm and Hörz [13]
21.2	−33.3	−38.6	−66.5	Wenzl [14]
21.1	−35.5	−37.9	−67.3	Used in present work

*For symbol definitions see text.
†Not used for the calculation of mean ΔH_1.

place as the temperature is lowered, which agrees with what is found experimentally. The effective hydrogen pressure in the system at the solvus temperature of 315° C will correspond to the dissociation pressure of the hydride, which from Equation 3 is 0.2 MPa at 315° C.

3.7. Precipitation and growth of magnesium hydride

Quenching to room temperature (15° C) from 580° C will produce a large hydrogen supersaturation. The dissociation pressure of the hydride at 15° C is 1.9×10^{-8} MPa and the limiting solubility is 4.19×10^{-5} ml per 100 g. Hydride is therefore very likely to form even with a rapid quench, unless the diffusion kinetics are very unfavourable. The formation of MgH_2 requires an expansion in volume of about 30%, which must be accommodated by self-diffusion in the magnesium matrix. Hydrogen diffuses rapidly in magnesium even at room temperature [22], and movement over a distance of about 0.5 μm could occur in 1 sec. For magnesium the lattice self-diffusion at 15° C is negligible [23], but with the reduced activation energy for grain boundary movement, diffusion could take place over a distance of 10^{-6} cm in a few minutes. This suggests therefore that limited formation of small hydride particles is likely to occur at grain boundaries in quenched material, and these may be responsible for the fine dimples observed on the grain boundary fractures of quenched samples.

Heating as-quenched material to 250° C will raise the hydride decomposition pressure to 0.03 MPa and the limiting solubility to 2.69 ml per 100 g. In addition, the increased diffusion rate of hydrogen at 250° C will enable hydrogen present inside the grains to diffuse rapidly to grain boundaries, to produce growth of the small hydride particles formed at room temperature. The typical grain size of the Magnox was approximately 350 μm, and at 250° C hydrogen could diffuse from a grain centre to a grain boundary in about 75 sec. Grain boundary self-diffusion of magnesium could occur over distances of about 2 μm in the same time. The diffusion kinetics would thus be favourable for precipitation of all the hydrogen in supersaturation and rapid growth of the initial hydride precipitates, in the first few minutes of heating at 250° C. Subsequently Ostwald ripening would occur with an increase in maximum particle size as shown by the fractographs and Fig. 5. However, at any particular stage of the ageing, the precipitates showed a range of sizes and with continued heating the larger ones would grow further and the smaller ones shrink. This is one possible explanation of the presence of small particles on the fracture surfaces at longer times of heating, e.g. after seven days of heating as in Fig. 6a. Such particles would still generate voids on the fracture surface but the voids would have to expand further to link up with adjacent voids, and hence result in regions on the fracture surface where the particles were much smaller than the voids.

A further observation was the presence of empty voids on the fracture surfaces, particularly with longer times of ageing. On average on any fracture surface, half the voids should be empty, with the missing particles on the other half of the fracture, assuming that they do not fracture. Also larger particles are more likely to fall out of the fracture surfaces. These reasons could explain the voids observed with the longer times of ageing at 250° C.

When material aged at 250° C was reheated to 350 or 450° C for 2 h, empty voids were again observed on fracture surfaces. The hydrogen solubility at these temperatures is in excess of the hydrogen present. Thus hydride particles would not be present after 2 h of heating, so particle loss could not explain the empty voids. The sample heated for the shorter time of 10 min at 350° C showed residual small hydride particles in larger voids. The most likely explanation of these effects is that they are due to thermal decomposition of the hydride, occurring at a faster rate than solution of hydrogen in the matrix. Complete dissociation of a hydride particle would result, due to density differences, in a void with a radius of 0.38 of that of the original particle, containing hydrogen at the dissociation pressure operative at the temperature of heating. Such voids could then be expanded by plastic deformation during fracture, and also possibly by plastic or creep deformation during the heating and induced by the internal gas pressure in the void. The hydrogen solubility at 250° C is considerably less than the hydrogen content of the Magnox and hence dissociation of the hydride would not be expected. Nevertheless the appearance of empty voids or voids containing small particles, after longer times of heating at 250° C, could be associated with void growth by a boundary creep mechanism due to the hydrogen pressure in equilibrium with the hydride. Further work on the influence of prolonged heating would be needed to test this possibility.

4. Summary and conclusions

In certain casts of Magnox AL80 the precipitates formed on some grain boundaries after a furnace-cool from the solution treatment temperature and/or after ageing at 250° C following a water-quench from the solution treatment temperature have been identified as magnesium hydride, MgH_2. This identification is based on electron diffraction evidence, LIMA results and the apparent dissociation behaviour of the precipitates to form a gas.

The solvus temperature for the grain-boundary hydride precipitates was deduced to be between 300 and 350° C. This temperature range can be correlated with the typical bulk hydrogen content, the variation with temperature of the hydrogen solubility in magnesium, and that of the dissociation pressure of MgH_2.

With longer times of ageing at 250° C cavities, in some cases associated with smaller precipitates, were found on fracture surfaces. Several possible explanations are put forward, including void expansion by creep deformation due to the hydrogen pressure over the hydride.

Cavities were also formed on some grain boundaries when hydride precipitation were reheated above the solvus temperature. Their formation appears to

result from the net effects of hydride dissolution and dissociation at the higher temperatures, and the volume decrease associated with hydride decomposition.

Acknowledgements

The authors would like to thank Professor R. W. K. Honeycombe FRS for the provision of laboratory facilities, and UKAEA Northern Division, Springfields for a maintenance grant to one of them (Y.P.L.) and for the supply of material. They also wish to thank Mr G. A. Burras, Mr. E. Ross and Mr R. A. Shaw of UKAEA, Springfields for many helpful discussions and assistance and, in particular, Mr Ross for permission to quote details of unpublished research results. Mr P. Georges is also thanked for his assistance with the precipitate growth experiments.

References

1. J. E. HARRIS, *Trans. Met. Soc. AIME* **233** (1965) 1509.
2. M. T. EVANS, unpublished research (1978).
3. B. LISOWYJ, PhD thesis, University of Leeds (1978).
4. J. E. HARRIS, *J. Nucl. Mater.* **15** (3) (1965) 201.
5. E. ROSS, unpublished research and private communication (1981).
6. F. H. ELLINGER, C. E. HOLLEY, B. B. McINTEER, D. PAVONNE, R. M. POTTER, E. STARITZKY and W. H. ZACHARIASEN, *J. Amer. Chem. Soc.* **77** (1955) 2647.
7. W. H. ZACHARIASEN, C. E. HOLLEY and J. F. STAMPFER, *Acta Crystallogr.* **16** (1963) 352.
8. T. SCHOBER, *Met. Trans.* **12A** (1981) 951.
9. T. SCHOBER and M. K. CHASON, *Scripta. Metall.* **15** (1981) 791.
10. Z. D. POPOVIC and G. R. PIERCY, *Met. Trans.* **6A** (1975) 1915.
11. Y. C. HUANG, T. WATANABE and R. KOMATSU, in Proceedings of 4th International Conference on Vacuum Metallurgy, Tokyo, 1973 (Iron and Steel Institute of Japan, Tokyo, 1973) p. 176.
12. J. F. STAMPFER, C. E. HOLLEY and J. F. SUTTLE, *J. Amer, Chem. Soc.* **82** (1960) 3504.
13. E. FROMM and G. HÖRZ, *Int. Met. Rev.* **25** (1980) 269.
14. H. WENZL, *ibid.* **27** (1982) 140.
15. R. FROMAGEAU, C. MAIRY and P. TZANETAKIS, *Scripta Metall.* **14** (1980) 395.
16. E. L. HUSTON, G. D. SANDROCK, *J. Less-Common Metals* **74** (1980) 435.
17. P. S. RUDMAN, *Scripta Metall.* **14** (1980) 1365.
18. A. C. CHAMI, J. P. BUGEAT and E. KIGEOU, *Rad. Eff.* **37** (1978) 37.
19. Z. D. POPOVIC and M. J. STOTT, *Phys. Rev. Lett.* **33** (1974) 1164.
20. E. F. EMLEY, "Principles of Magnesium Technology" (Pergamon, Oxford 1966).
21. A. E. VOL, "Handbook of binary metallic systems", Vol. 1 (US Department of Commerce and National Science Foundation, 1967).
22. J. RENNES and H. J. GRABKE, *Z. Metallkde* **69** (1978) 639.
23. A. NEEDLEMAN and J. R. RICE, *Acta Metall.* **28** (1980) 1315.

Received 29 June
and accepted 22 September 1987.